Numerical Investigation of a Dual Stage Variable Isp Ion Engine

IEPC-2011-204

Presented at the 32nd International Electric Propulsion Conference,
Wiesbaden • Germany
September 11 – 15, 2011

M. Coletti[1] and Stephen B. Gabriel[2]
Astronautics Research Group, University of Southampton, Southampton SO17 1DR, UK

In the frame of the HiPER project a parametric study has been performed over the ion optics of a dual stage ion engine. The goal of the study is to understand the effect the operational parameters of a dual stage ion engine over CEX ions production and ultimately over the thruster lifetime. In this paper the effects of the extraction voltage, acceleration voltage, extracted current and grid radius will be presented. After this a candidate DS3G design will be simulated at Isp level from 3500 to 10000 seconds and the result compared to the one of conventional ion engines.

I. Introduction

THE aim of the HiPER project is to define the roadmap for the future of electric propulsion [1]. To do so several missions are under study, including a Mars sample return mission, rendezvous with Near Earth Objects, building of infrastructure on the Moon-Earth L1 point and building of infrastructure on Mars.

Different electric propulsion subsystems are under study for these missions including Magneto Plasma Dynamic Thrusters (MPDTs), Hall Effect Thrusters (HETs) and Gridded Ion Engines (GIEs).

The University of Southampton and Mars Space Ltd are working on the design of GIEs and in particular of a new concept of GIE called Dual Stage Gridded Ion Engine originally developed by the late D. G. Fearn [2] based on tetrode extraction system for high energy neutrals and ions used in tokamaks [3-6].

In this paper the dual stage ion engine concept will be quickly presented together with some of the past results for then focusing on the study of the effect of the thruster operational parameters over its lifetime. Finally a candidate thruster design will be simulated at Isp levels from 3500 to 10000 s and compared to the performances of conventional GIE working at the same impulse levels.

II. The Dual Stage Ion Engine

Existing GIEs can provide specific impulses in the 2000-10000s range [7] with an experimental GIE able to achieve 19300s [8]. However, GIEs present an intrinsic compromise between maximum current density and specific impulse, which limits the maximum achievable thrust for a given specific impulse and hence the thrust density. This ultimately affects the maximum thrust achievable with a GIE since the maximum grid area is limited by the available space on the launcher and by the structural resistance of the grids. The reason for the thrust density limitation is basically that the ion extraction (that assuming a fixed electric field value decreases with increasing applied voltages) and the ion acceleration (that increases with increasing applied voltages) both take place in the gap between the first and the second grid. A solution to overcome this limitation has been envisioned by D. Fearn [2] and is based on multi stage ion optics commonly used for high energy particle injections in tokamaks [4-6, 9].

In a multi stage ion optics system the total voltage drop is divided over two or more gaps hence isolating the extraction process (that takes place in the first gap) from the acceleration process (that mainly takes place in the following gaps) allowing the achievement of high specific impulses (up to 15,000 s have been demonstrated at

---

[1] Post Doctoral Researcher, Astronautics Research Group, School of Engineering Sciences, coletti@soton.ac.uk
[2] Professor, Astronautics Research Group, School of Engineering Sciences, sbg2@soton.ac.uk

ESTEC [10] but beam energies up to 80kV are used in similar fusion devices) without the need of reducing the extracted current density and hence proportionally increasing the thrust density.

In the original concept developed by Fearn and built and tested at ESTEC by a collaboration between ESA and ANU [11] the dual stage ion engine presented four grids: the first one (screen grid) at very high positive potential, the second one (extraction grid) at slightly lower positive potential providing the extraction voltage drop, the third one (accel grid) at low negative potential to prevent electron backstreaming and to provide the acceleration voltage drop and the fourth one (earth grid) at ground potential.

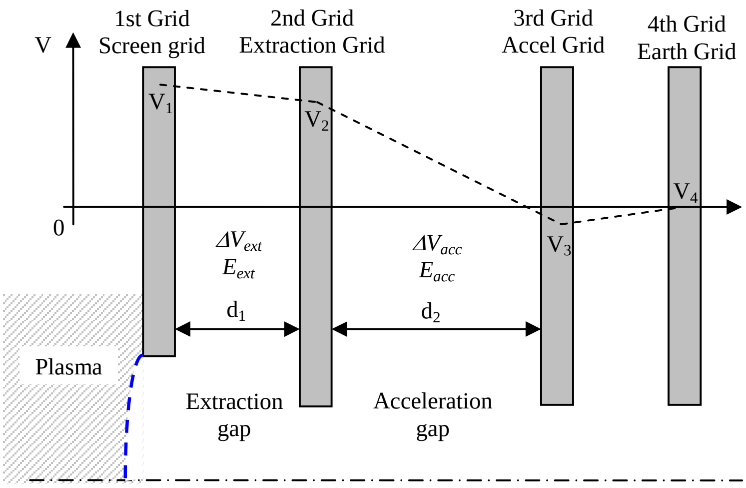

Figure 1. Schematics of a dual stage ion optics

Subsequent work by the authors [12] showed how the use of a fourth grid is non-necessary and, as in conventional GIE, the increase in complexity relative to its presence will probably overcome the benefits obtained from it. Since we moved from a 4 gridded to a 3 gridded dual stage ion engine we will from now one refer to it as DS3G.

Another advantage of a dual stage ion engine is the possibility of achieving very low jet divergence thanks to the presence of an extra grid and hence of an extra electrostatic lens. Nevertheless in [12] using the analytical model reported in [13] and the IGX code [14] it has been show how, if a well collimated jet is desired (ideally with no divergence), an interdependence exists between the extraction and the acceleration process. In particular a relationship between the ratio of the voltage in the second gap (acceleration voltage) to the one in the first gap (extraction voltage) Γ and the optimal critical perveance ratio P/P_0 defined as the ratio between the working perveance and the Child-Langmuir limited perveance has been reported as a function of the ratio between the first and second gap spacing λ. From this a relationship between the thrust density and Γ has been derived (Figure 2) [12].

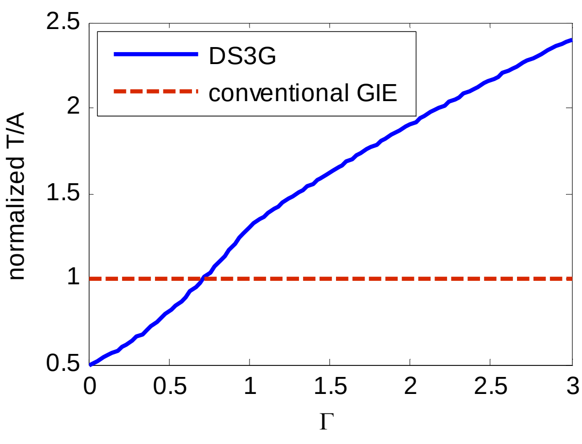

Figure 2. DS3G thrust density trend with Γ [15]

As it can be seen from Figure 2 the DS3G theoretically offers advantages over a conventional GIE in terms of thrust density only if the voltage difference applied in the second stage is 0.6 times the one in the first stage or bigger. Assuming that the extraction stage will work with an extraction voltage drop of about 2000 V (in agreement with what is found in commercial GIE [7]) the DS3G will offer advantages only for Isp values of 6,000s and above.

Using the results obtained in [12] a full DS3G ion optics have been designed to provide an Isp of 10,000s and a thrust density in excess of 10 N/m^2. The lifetime of such thruster have been evaluated using the FFX code developed at CSU [16-18] and compared to the one of a typical two grid GIE (TypGIE) having the same extraction voltage drop, extracted beam current and accel grid potential [19]. It was found that, thanks to the presence of an extra grid the CEX ions that normally would in pact on the accel grid of a typical GIE in a DS3G are "split" between the extraction and accel grid hence producing lower erosion rates ultimately resulting in longer lifetime.

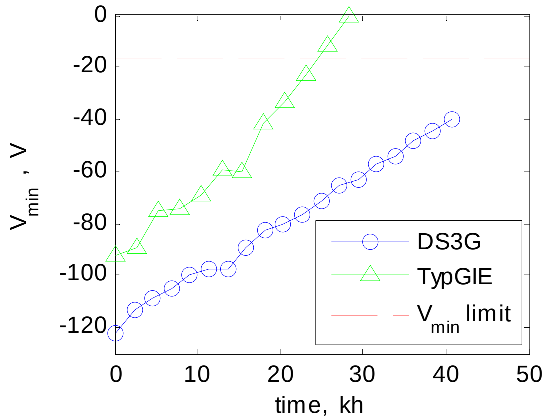

Figure 3. Trend of the minimum centerline potential with time for the DS3G and the TypGIE [19]

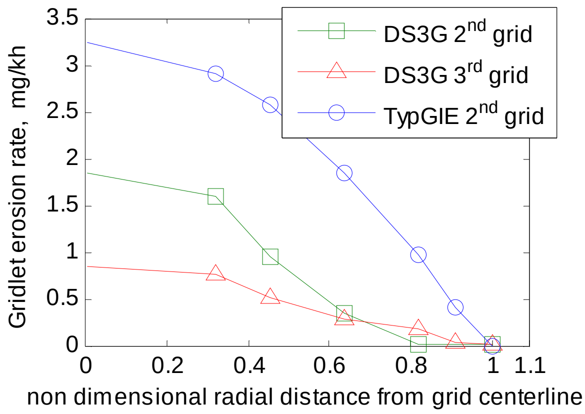

Figure 4. Gridlet erosion rate for the TypGIE and the DS3G [19]

In conclusion the DS3G was found to be able to provide higher Isp and higher thrust density than a conventional GIE without suffering any penalty in term of lifetime.

III. The Numerical Study

In the last year a parametric numerical study of the influence of the design and operational parameters over the DS3G performance has been carried out [20, 21] with the aim of increasing the understating of the thruster and of exploring its capabilities. One of the main findings of this study was that the DS3G, thanks to the presence of two ion optics stages, has the possibility of working at various Isp levels [20]. It was also observed how the Isp has a strong influence on lifetime with higher Isp levels producing lower sputtering rates hence longer lifetimes [21].

Table 1. DS3G and GIE lifetime [21]

Thruster	Isp [s]	Lifetime [h]	Cause of failure
DS3G	5,000	7,000	Grid erosion
	6,000	4,000	Grid erosion
	7,000	12,000	V_{min}
	8,000	15,000	V_{min}
	10,000	33,000	V_{min}

A deeper analysis of these data showed how the reason for this trend of lifetime with Isp is the different CEX ions focusing at the various specific impulse levels. This can be better visualized looking at the CEX ions production maps and the CEX ions impact energy distribution reported in the figures below.

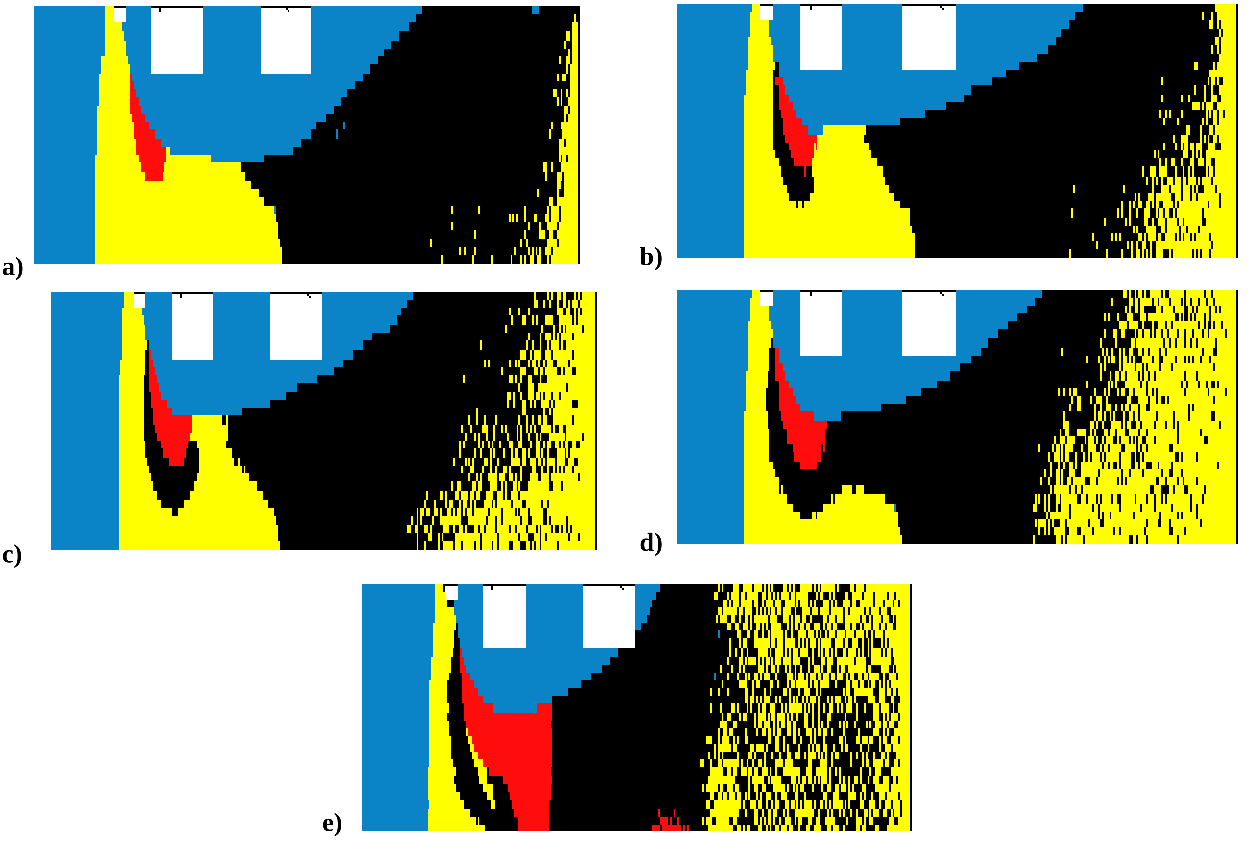

Figure 5. DS3G CEX ions production map for different Isp levels a)10,000s b)8,000s c)7,000 d)6,000 e)5,000s. The CEX produced red area will impact the second grid, the one in the black are will impact the third grid whereas the ones in the yellow area will be accelerated downstream.

As it can be seen from the maps reported in Figure 5, at 10,000s no CEX ions produced close to second grid impacts the accel grid whereas decreasing the Isp the amount of charge exchange ions reaching the third grid keeps increasing getting to the point where, at 6,000s, all the CEX produced in the second gap and a sensible fraction of those produced in the first gap impact on the accel grid. The increase of CEX focusing is reflected also in Figure 6 where it can be seen how at higher Isp the CEX energy distribution has a very strong peak at about 250V (equal to the accel grid voltage and hence corresponding to the energy of the CEX ions coming from the downstream plasma) and almost no CEX ions are produced at high voltage, whereas, decreasing the Isp, the intensity of the 250V peak is reduced with a growing presence of high voltage (more than 1keV) CEX ions.

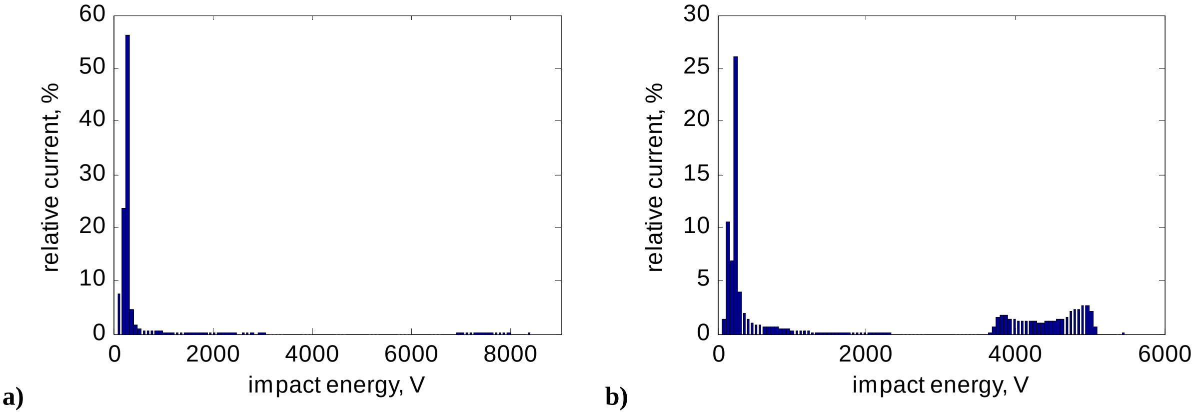

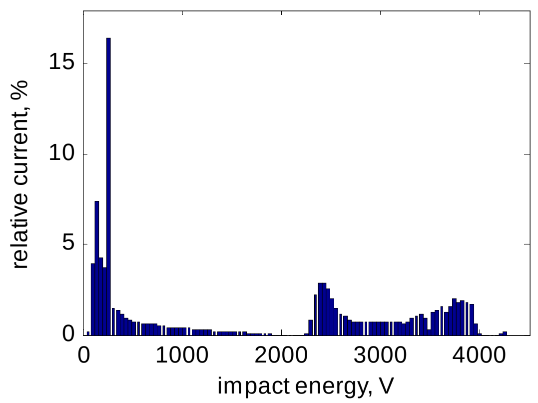

c)

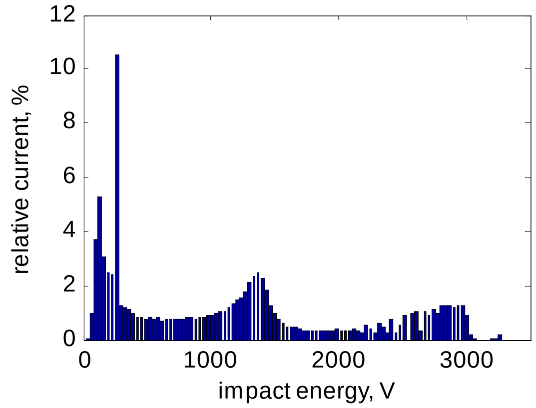

d)

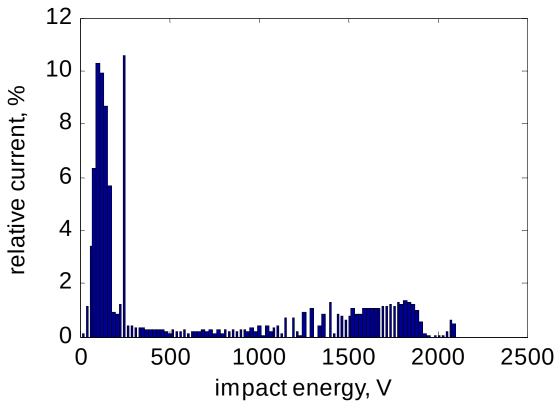

e)

Figure 6. DS3G accel grid CEX ions energy distribution for different Isp levels a)10,000s b)8,000s c)7,000 d)6,000 e)5,000s.

The ultimate effect of the better focusing of the charge exchange ions at high Isp levels are lower flux to the accel grid and lower mean CEX impact energy hence resulting in lower erosion rates hence in sensibly longer lifetime as reported in Table 1. To extend the range of operation of the DS3G it would be beneficial to be able to obtain the same CEX focusing achieved at 10,000 at lower Isp levels.

The aim of this paper is to study the influence of the thruster operational parameters over the CEX focusing with the aim of producing a DS3G design able to deliver long lifetime over a wide range of specific impulses.

To do so the parameters that influence the CEX focusing need to be clearly identified and their effect studied in detail. The factors that may influence the CEX focusing are:

a) the beamlet current level in the first stage
b) the grid aperture size
c) the specific impulse level (beam voltage)
d) the ratio between the voltage drop/electric field in the first stage and the one in the second stage

To study the influence of these parameters simulations have be run using the FFX code developed at CSU [16-18] at 7000, 8000 and 10,000s Isp for several different DS3G configuration. The different parameters used in the simulations have been reported in Table 2.

Table 2. DS3G geometrical dimensions and operational parameters

Screen grid aperture radius (r_1)	0.8 mm	0.9 mm		1 mm
Extraction grid aperture radius (r_2)		80% r_1		
Accel grid aperture radius (r_3)		80% r_1		
Extraction Voltage (ΔV_{ext})	1250V	1500 V	1750 V	2000 V
Accel Grid Potential		-250 V		

Screen grid thickness (t_1)	~0.5 mm		
Extraction grid thickness (t_2)	1 mm		
Accel grid thickness (t_3)	1.3 mm		
Grids material	molybdenum		
Acceleration stage gap (d_2)	0.35 – 2.34 mm (1.5mm nominal)		
Beamlet current	0.2 – 0.4 mA (0.3 mA nominal)		
Specific Impulse (Isp)	7000 s	8000 s	10000s

The CEX focusing will be judged based on two parameters. The first is the mean sputtering charge exchange ions impact energy (E_{CEX}) the second one is the fraction of the CEX current impacting with energy in excess of 2keV (I_{2keV}).

A. Beamlet current level

The beamlet current used clearly influence the focusing of the ion beam and consequently the CEX production zones. Higher beamlet current levels will produce flatter sheath shape producing larger ion beams hence potentially creating CEX ions further away from the gridlet axis whereas lower currents will produce more curved sheath shape and a more focused and narrow ion beam hence limiting the CEX production area extension in the radial direction.

To investigate this effect a DS3G presenting an acceleration stage gap of 1.5mm and an extraction voltage of 2000V has been simulated at the Isp levels reported in Table 2 for several beamlet current levels. The result of these simulations are reported below

Table 3. Beamlet current effect on CEX focusing

Isp	Beamlet current [mA]	P/P_0	Mean CEX Impact Energy E_{CEX} [V]	CEX Current over 2keV I_{2keV} [%]
10,000	0.22	0.53	354	5
	0.25	0.61	283	2.2
	0.28	0.67	286	1.7
	0.30	0.73	293	1.8
	0.32	0.79	320	2
8,000	0.22	0.53	1634	46
	0.25	0.61	1570	45
	0.28	0.67	1397	40
	0.30	0.73	1387	39.2
	0.32	0.79	1375	38.1
	0.35	0.85	1342	36.4
7,000	0.22	0.53	1492	56.3
	0.25	0.61	1433	53.8
	0.28	0.67	1391	51.6
	0.30	0.73	1328	48.3
	0.32	0.79	1242	43.8
	0.35	0.85	1231	42.3

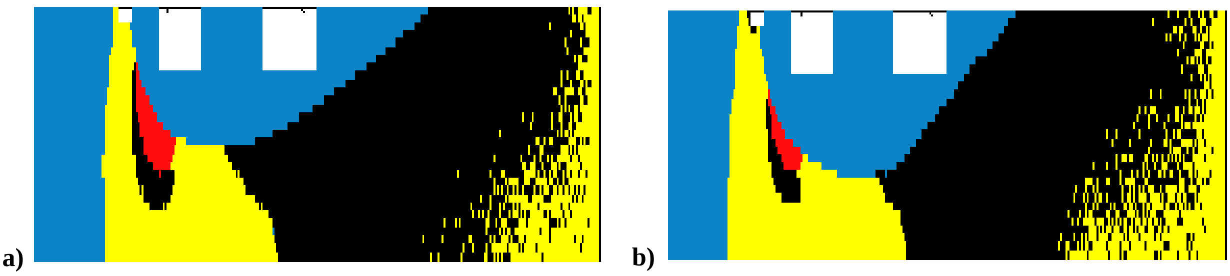

Figure 7. DS3G CEX ions production map. Isp=8000s a) $I_{beamlet}$ =0.35mA, b) $I_{beamlet}$=0.22mA

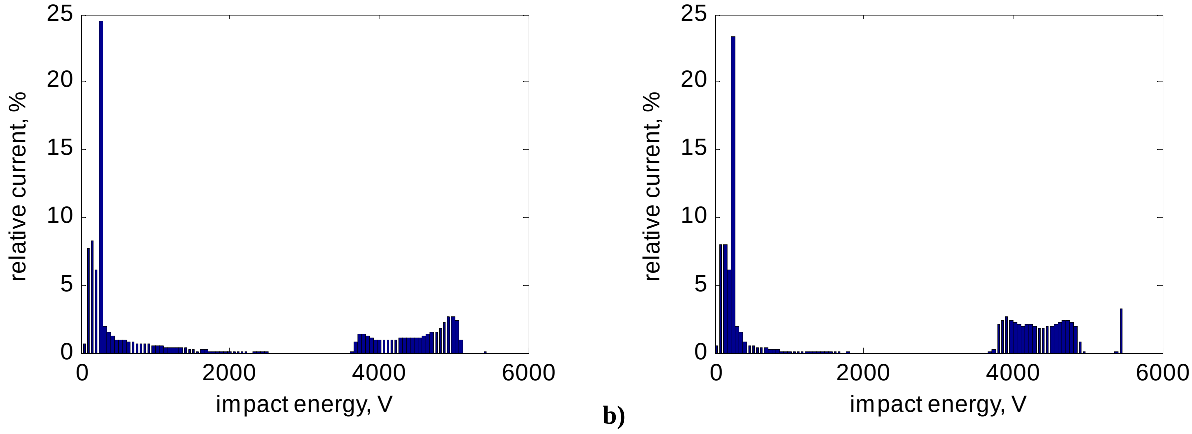

Figure 8. DS3G accel grid CEX ions energy. Isp=8000s a) $I_{beamlet}$ =0.35mA, b) $I_{beamlet}$=0.22mA

As it can be seen at 7000 at 8000 s and increase in beamlet current helps improving the CEX focusing decreasing both the value of E_{CEX} and of I_{2keV} whereas in the 10000s case the trend presents an optimum at about 0.28 mA.
In Figure 7 and 8 it can be noted how at low current levels a very small fraction of the CEX ions created close the screen grid managed to impact on the accel grid hence generating the high energy peak in Figure 8 b).
It can be concluded that while the beamlet current has an effect on the CEX focusing this depends on the Isp level and is not very strong hence not being the main driver for CEX focusing.

B. Grid aperture radius

Another parameter that might affect the CEX focusing is the beamlet radius. Predicting the effect of the radius on the CEX focusing is difficult since smaller radii should produce stronger radial fields hence helping the CEX focusing but in turn smaller apertures means also that a CEX generated on the axis needs to travel a smaller radial distance before impacting on a grid. To judge this effect the 7000. 8000 and 10000 Isp cases have been simulated for the three radii reported in Table 2 keeping the upstream plasma density constant hence working with the same extracted current density.

Table 4. Aperture radii effect on CEX focusing

Isp	Screen grid radius [mm]	Mean CEX Impact Energy E_{CEX} [V]	CEX Current over 2keV I_{2keV} [%]
10,000	1.2	326.6	1.6
	1	286	1.7
	0.8	360	5
8,000	1.2	1361	37
	1	1387	39.2
	0.8	1405	41
7,000	1.2	1030	36.6
	1	1328	48.3
	0.8	1414	54

As it can be seen from Table 4 the effect of the aperture radius over E_{CEX} and I_{2keV} is quite modest for the 8000 and 10000 s case whereas it is more marked for the 7000s case with larger apertures proving lower mean impact energy and lower high energy current fraction. Nevertheless it must be noted that a larger aperture radius will produce an increase in the minimum centerline potential hence reducing the margin over the incurrence of electron backstreaming.

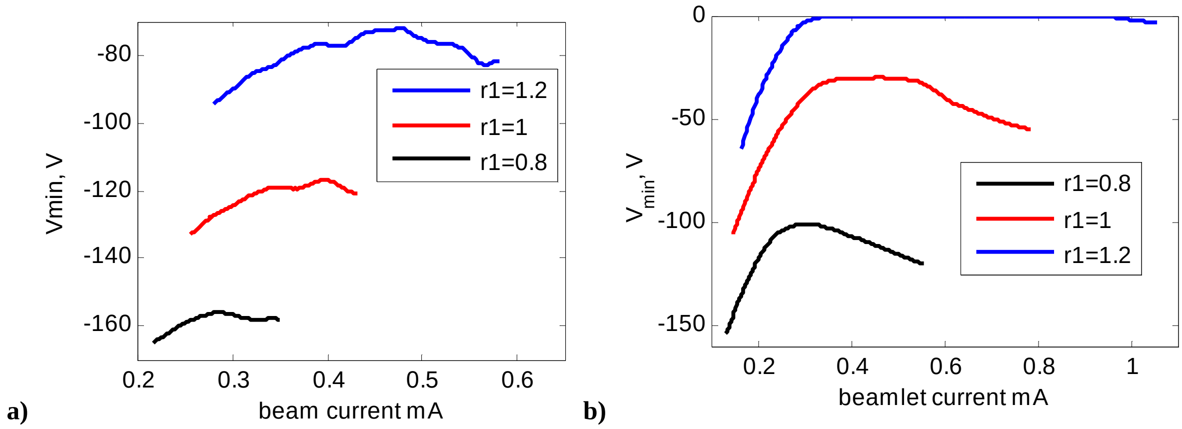

Figure 9. Minimum centerline potential trend for different aperture radii and Isp levels. a) 7000s, b) 8000s.

Comparing the data reporter in Table 4 and Figure 9 it can be seen how the effect of the aperture radius over V_{min} overweigh the one over E_{CEX} and I_{2keV} hence for the design of a variable Isp ion engine the use of smaller (either 0.8 or 1 mm) aperture radii will be preferred.

C. Specific impulse (beam voltage) effect

One of the possible causes of the change in CEX focusing at different Isp levels might be the effect that the use of higher beam voltages could have on the perveance of the first stage. The higher the beam voltage the bigger the potential difference between the second and third grid hence the more likely the possibility that the presence of the extra third grid will modify the voltage distribution in proximity of the extraction grid aperture, locally decreasing the potential value, and hence increasing the electric field in the first gap. An electric field increase in the first gap would result in an augmented perveance and hence, given the fact that in these simulations the beamlet current is kept constant, in a more focused ion beam with an effect over the CEX focusing correspondent to what reported in Sec. III.B

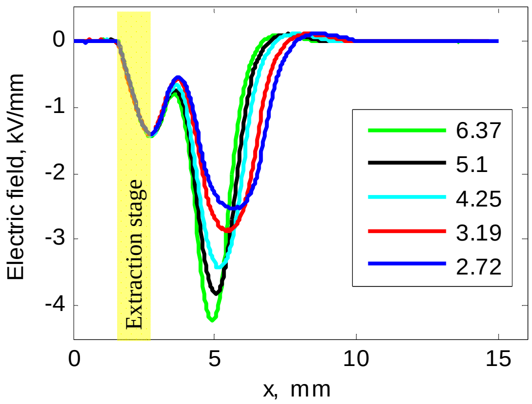

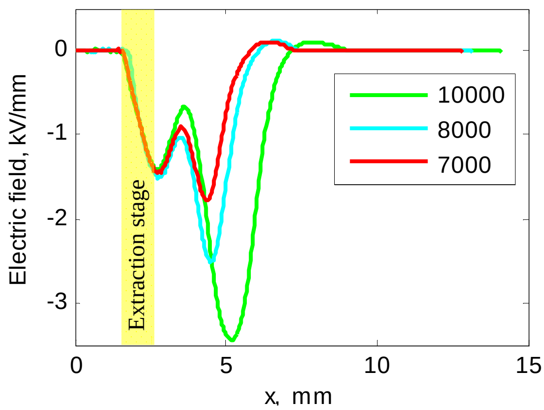

Figure 10. E field trend along the gridlet centerline at 10,000s for different accel stage gaps.

Figure 11. E field trend along the gridlet centerline at different Isp levels for a E_{nom} = 4.25 kV/mm

In Figure 10 and 11 the trend of the electric filed along the gridlet centerline at various Isp levels and for various acceleration stage gaps has been reported. In all these cases the electric field trend in the first stage does not change appreciably hence leaving the perveance of the system unchanged. These results show how the acceleration stage gap and the beam voltage do not influence the extraction process and hence how the change in CEX focusing is not due to a change in the perveance of the ion optics extraction stage at higher Isp. It can be concluded that the Isp level alone is not the cause of better CEX focusing.

D. Second to first stage electric field/voltage drop ratio

One of the strongest candidates to be the main driver of CEX focusing is the ratio between the electric fields and the voltage drops in the second and first stage. This is due to the fact that the both these parameters will influence the focal length of the electrostatic lens corresponding to the second grid [13, 22] hence changing the "strength" of the extraction grid focusing effect. To study this effect we will first define the ratios as $\Psi = E_{acc}/E_{ext}$ and $\Gamma=\Delta V_{acc}/\Delta V_{ext}$ where the acceleration electric field is $E_{ext}=\Delta V_{acc}/[d_2+(t_2+t_3)/2]$ and the extraction one $E_{ext}=\Delta V_{ext}/l_e$ and where l_e is the equivalent extraction stage gap defined as

$$l_e = \sqrt{(d_1 + t_1 + t_2/2)^2 + r_1^2} \tag{1}$$

Several simulations have been run varying the acceleration stage gap and voltage drop and the extraction stage voltage drop at the usual Isp levels of 7000, 8000 and 10000. In the simulations where the extraction stage voltage drop has been changed the extracted current has been changed accordingly to keep the perveance constant.

Table 5. Γ and Ψ effect on CEX focusing

Isp [s]	ΔV_{ext} [V]	ΔV_{acc} [V]	d_2 [mm]	$\Gamma=\Delta V_{acc}/\Delta V_{ext}$	$\Psi = E_{acc}/E_{ext}$	E_{CEX} [V]	I_{2keV} [%]
10000	2000	6370	1	3.19	2.67	262	0.62
	2000	6370	1.25	3.19	2.39	272	0.8
	2000	6370	1.5	3.19	2.17	293	1.8
	2000	6370	2	3.19	1.82	367	4.7
	2000	6370	2.14	3.19	1.75	562.5	11.3
	2000	6370	2.34	3.19	1.65	532	11.2
8000	2000	3450	0.54	1.73	1.84	426	3.1
	2000	3450	0.67	1.73	1.71	558	9.6
	2000	3450	0.8	1.73	1.59	750	17
	2000	3450	0.96	1.73	1.47	873	21.8
	2000	3450	1.08	1.73	1.39	940	23.8
	2000	3450	1.28	1.73	1.28	1150	29.2
	2000	3450	1.5	1.73	1.17	1387	39.2
	1750	3700	1.5	2.11	1.44	913	27.8
	1500	3950	1.5	2.63	1.44	621	14.2
	1250	4200	1.5	2.63	1.79	311	4.27
7000	2000	2250	0.35	1.13	1.35	724	26.6
	2000	2250	0.49	1.13	1.24	828.47	31.2
	2000	2250	0.52	1.13	1.21	824	31.3
	2000	2250	0.61	1.13	1.15	926.5	35.1
	2000	2250	0.74	1.13	1.07	1014	38.2
	2000	2250	0.82	1.13	1.03	1054	39.3
	2000	2250	0.98	1.13	0.95	1121	42
	2000	2250	1.15	1.13	0.88	1192	44.2
	2000	2250	1.15	1.13	0.77	1328	48.3
	1750	2500	1.5	1.43	0.97	1105	37
	1500	2750	1.5	1.83	0.97	1151	42
	1250	3000	1.5	1.83	1.25	877	26

As it can be seen from Table 5 there seems to be a clear trend of CEX focusing with Ψ with its increase producing a constant improvement of the E_{CEX} and I_{2keV} values in all cases except for d_2 =2.14 mm at 10000s. For what instead concerns the ratio of the voltage drops it can be seen how different values of E_{CEX} and I_{2keV} have been obtained in simulations run at the same Isp and Γ level (e.g. 10000s case in Table 5) hence bringing to the conclusion that Γ is not the driver for CEX focusing.

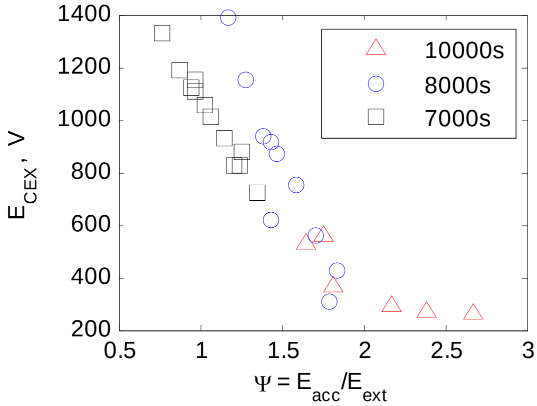

Figure 12. Mean CEX impact energy trend with ratio of electric fields for different Isp levels

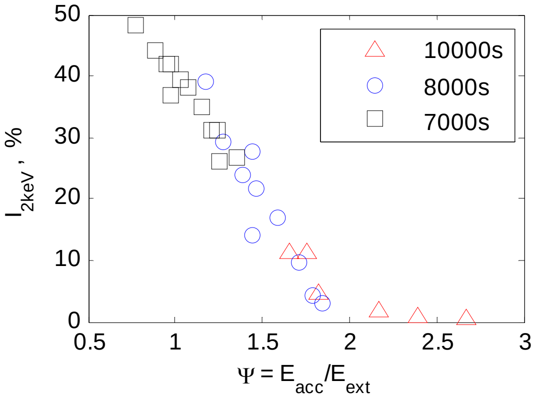

Figure 13. I_{2keV} impact energy trend with ratio of electric fields for different Isp levels

Looking at Figure 12 and 13 it can be seen how the values of I_{2keV} relative to the different Isp levels all obey the same linear regression until about Ψ=1.7 from which the amount of CEX impacting with energy over 2 keV goes to zero. For what concerns E_{CEX} also its value becomes constant for a electric field ratios over 1.7; in this case the constant value corresponds to the accel grid voltage (-250 V) representing the CEX ions produced in the downstream plasma that backstream to impact on the accel grid. Moreover it can be noted that the E_{CEX} values relative to the three Isp level all obey linear regressions until Ψ=1.7 but with a steeper E_{CEX} decrease for higher Isp. This is due to the fact that the higher the Isp the higher the beam voltage hence the larger the energy CEX ions can gain before impacting on the accel grid. To eliminate this effect the impact energy of the CEX ions will be normalized using the beam voltage values and plotted as a function of Ψ

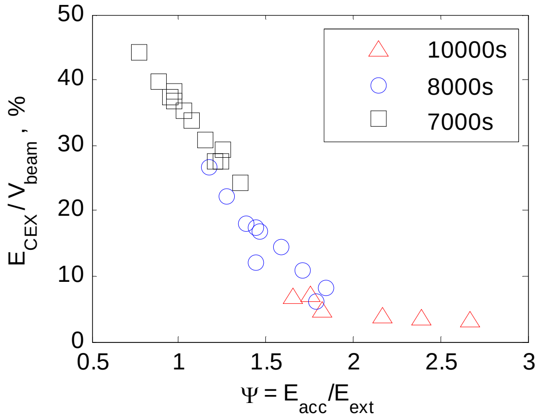

Figure 14. Trend of the ratio between E_{CEX} and the beam voltage with ratio of electric fields for different Isp levels.

As it can be seen once the value of E_{CEX} is normalized to the beam voltage value all the point relative to the three Isp level under study collapsed on the same regression as already observed for I_{2keV}. From the data reported in Table 5 and in Figure 13 and 14 it can be then concluded that the main driver for the CEX focusing is the ratio between the extraction and acceleration electric fields.

IV. Variable Isp DS3G design attempt

Now that the main parameter responsible for the CEX ion focusing has been identified to be the ratio of the electric fields Ψ an attempt in designing the ion optics of a DS3G able to work on a wide range of specific impulse levels will be performed. Ideally a high value of Ψ must be employed, this means that, assuming to keep the grid spacing constant, most of the voltage drop should take place in the acceleration stage; nevertheless a decrease in the extraction voltage drop will cause a decrease in the extracted current density with a proportional reduction in thrust density hence a trade-off between lifetime (CEX focusing) and thrust density should be done.

Expressing the extracted current density as

$$J = \frac{4\varepsilon_0}{9}\sqrt{\frac{2q}{M}}\frac{E_{ext}^2}{\sqrt{\Delta V_{ext}}} \tag{2}$$

and the Isp as

$$Isp = \frac{1}{g_0}\sqrt{\frac{2q}{M}\left(\Delta V_{ext} + \Delta V_{acc} - |V_{acc}|\right)} \tag{3}$$

the thrust density becomes

$$T/A = \frac{8\varepsilon_0}{9}E_{ext}^2\sqrt{1 + \frac{\Delta V_{acc} - |V_{acc}|}{\Delta V_{ext}}} \tag{4}$$

Now taking into account that the electric field in any of the gaps is limited by the occurrence of arcing to a value of about 4 kV/mm and assuming an extraction stage gap of 0.5mm and acceleration stage gap of 1.5mm and the grid thicknesses reported in Table 2 the trend of the thrust density T/A and of the electric field ratios Ψ with the specific impulse has been calculated for different values of the extraction voltage ΔV_{ext}.

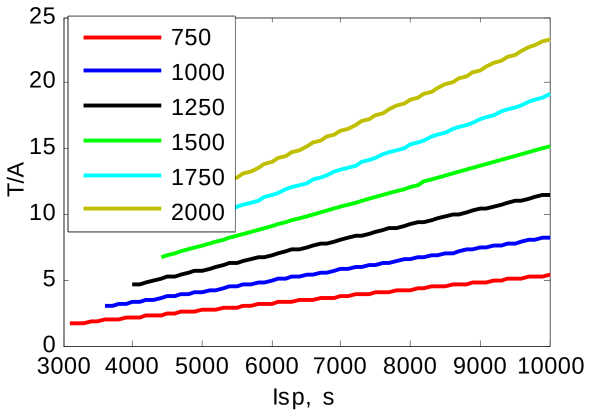

Figure 15. Thrust density trend with Isp for different extraction voltages

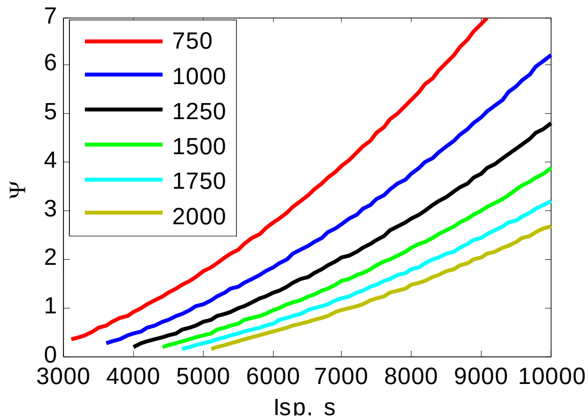

Figure 16. Electric field ratio Ψ trend with Isp for different extraction voltages

As it can be seen from Figure 15 and 16 higher extraction voltages will allow for higher thrust densities but at the same time will produce lower values of Ψ hence limiting the use of the DS3G to higher levels of Isp if long lifetime is required.

In the light of designing a variable Isp dual stage ion engine and at the same time verifying that working at higher Ψ values will enhance the DS3G lifetime we have decided to use an extraction voltage of 1000V together with the stage gaps reported above and the grid thicknesses reported in Table 2. The screen grid aperture will be 1 mm in radius and the extraction and accel grid one will be 80% of that. The optics will be numerically simulated with the FFX code [16-18] to evaluate its lifetime at 3500, 5000, 6000, 7000, 8000 and 10,000s, the results so obtained will be compared to those relative to a conventional 2 gridded GIE (from now on simply GIE) working at 3500 and 5000s. The GIE will not be tested at voltages in excess of 5000s since over this value the electric field in the grid gap will go appreciably over 4 kV/mm sensibly increasing the risk of arcing. Both thrusters will extract a beamlet current of 0.18 mA.

A. Lifetime simulation results

The lifetime of the DS3G and GIE will be assesses looking at both the trend of the minimum centerline potential and at the trend of the grids mass. The ion optics will be considered to have reached their end of life when ether the value of V_{min} goes over the backstreaming limit (calculated assuming a maximum electron backstreaming current of

1% of the beamlet current and an electron temperature in the beam plasma of 2eV [7]) or when the grid mass is reduced to 10% of its initial value.

The trend of the minimum centerline potential and of the accel grid mass is reported in the figures below together with the various lifetimes in

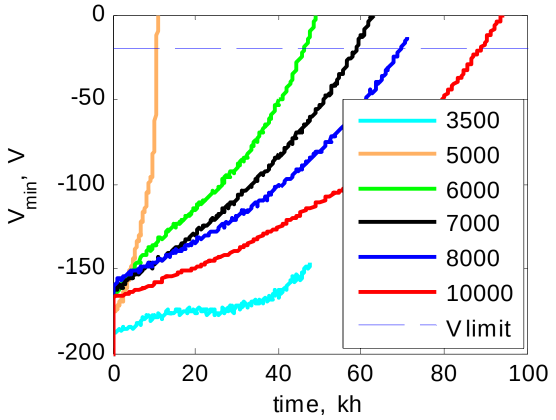

Figure 17. Minimum centerline potential trend at various Isp level for the DS3G

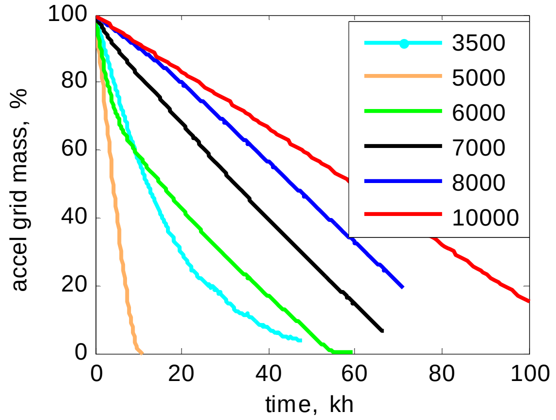

Figure 18 Accel grid mass trend with lifetime at various Isp level for the DS3G

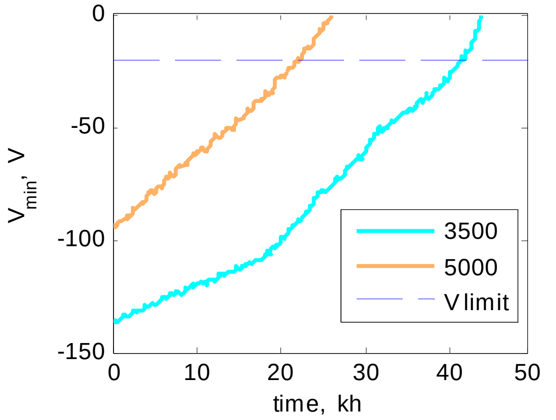

Figure 19. Minimum centerline potential trend for the GIE at different Isp level

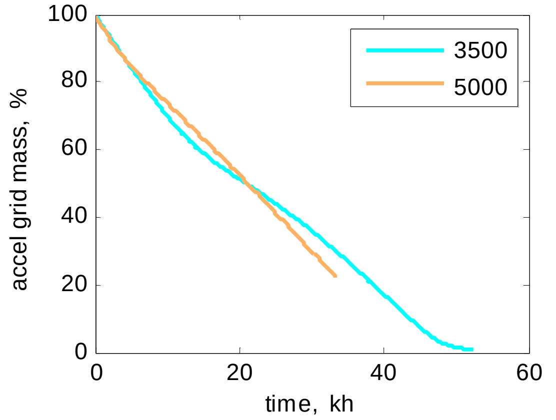

Figure 20 Accel grid mass trend with lifetime at various Isp level for the GIE

Table 6. DS3G and GIE lifetimes at different Isp

	Isp, [s]	Ψ	$E_{CEX}/\Delta V_{acc}$	Lifetime, [h]	T/A, [N/m^2]
DS3G	3500	0	-	40,000	2.14
	5000	0.40	76.0	10,000	3.06
	6000	0.98	42.7	47,000	3.67
	7000	1.47	20.9	60,000	4.28
	8000	2.05	5.9	70,000	4.89
	10000	3.48	2.8	90,000	6.11
GIE	3500	-	-	40,000	2.14
	5000	-	-	20,000	3.06

As it can be seen from Figure 17 and 18 and from Table 6 the lifetime of the DS3G presents a minimum at 5000s with only 10,000 hours. This can be explained noting the high average impact energy and the low ratio of the electric fields. At 3500 and the DS3G lifetime is the same as the GIE one whereas at 5000s it is half of the one produced by the GIE. From 6000 onwards the DS3G lifetime increase constantly up to 90,000 hours, more than twice the GIE value at 3500s and five times the value of 5000s. It should also be noted how, in agreement with what found in Sec. III.D, the longest lifetime are achieved when the value of Ψ increase above 1.7 hence confirming that to obtain long lifetime at different Isp level a dual stage ion engine need to be designed to have the highest possible value of Ψ across the specific impulse level of interest.

Looking at Table 6 it must also be noted how, due to the reduction in the extraction voltage, and of the correspondent reduction in extracted current density, the thrust density ranges between the values of 2 and 6 well below the 15 N/m^2 achieved at 10,000 by the dual stage ion engine simulated in [19]. Nevertheless it must be noted how the reported values of T/A are still on the high end of those achieved by conventional GIE as it can be seen from Table 7

Table 7. Main performance parameters for ion thrusters

	Power, [kW]	Thrust, [mN]	Beam Area, [cm^2]	Thrust Density, [N/m^2]	Specific Impulse, [s]
HiPEP [23]	39.3	670	3730	1.8	9620
NEXIS [24]	23.2	475	2550	1.9	7500
NEXT [25]	6.9	237	1020	2.3	4180
25-cm XIPS [7]	4.3	166	490	3.4	3550
NSTAR [7]	2.3	93	640	1.5	3130
JAXA [26]	4.6	210	960	2.2	3500
T6	~ 6	210	380	5.5	4700
RIT 22 [27]	~ 9	250	350	7.1	6400
RIT XT [28]	8.1	218	350	6.2	6420

V. Conclusions and Future Work

A numerical study has been conducted on a dual stage ion engine ion optics to determine the main factors that influence the charge exchange ion focusing. It has been found that the main driver of CEX focusing is the ratio between the electric filed applied in the acceleration stage to that applied in the extraction stage. In particular values of Ψ in excess of 1.7 have proven to minimize the mean CEX impact energy hence reducing erosion rates and enhancing lifetime. The radius of the grid apertures has also been found to play a role in CEX focusing with smaller radii providing better focusing and lower impact energies. The beam voltage alone has found not to influence the CEX focusing and moreover it has been clearly shown how the entity of the extraction stage voltage drop/electric field does no influence the electric field in the extraction stage and hence the maximum perveance of the system confirming the statement according to which in a dual stage ion optics the extraction and acceleration process are decoupled.

Using the results of the numerical study a candidate DS3G design able to work at various Isp levels has been numerically simulated at specific impulse of 3500, 5000, 6000, 7000, 8000, 10000 and the results compared to those relative to a conventional GIE having an equivalent ion optics geometry.

The results showed how the DS3G lifetimes are similar, even if slightly lower, to the one produced by the GIE at Isp level of 3500 and 5000s. At higher Isp level s the DS3G lifetime are sensibly longer achieving 90,000 hours at 10,000s.

Acknowledgments

The research leading to these results has received funding from the European Community's Seventh Framework Programme (FP7/2007-2013) under grant agreement n° 218859.

The authors would also like to thank Prof John Williams and Dr. Cody Farnell from CSU for the help with the FFX code.

References

[1] C.Casaregola, G.Cesaretti, and M.Andrenucci, "*HiPER: a Roadmap for Future Space Exploration with innovative Electric Propulsion Technologies*", 31st International Electric Propulsion Conference,University of Michigan, Ann Arbor, Michigan, USA, September 20 - 24, 2009

[2] C.Bramanti and D.Fearn, "*The Design and Operation of Beam Diagnostics for the Dual Stage 4-Grid Ion Thruster* ", 30th International Electric Propulsion Conference, Florence, Italy September 17-20, 2007

[3] J.R.Coupland and E.Thompson, "*The Production of High Current, High Quality Beams of Ions and Neutral Particles*", The Review of Scientific Instruments, Vol 42, No 7, 1971

[4] J.Kim, W.L.Gardner, and M.M.Menon, "Experimental study of ion beam optics in a two-stage accelerator," *Review of Scientific Instruments*, Vol. Vol 50, No. Iss 2, 1979, pp. 201-206.

[5] A.R.Martin, "High power beams for neutral injection heating," *Vacuum*, Vol. 34, No. 1-2, 2001, pp. 17-24.

[6] Y.Okumura, S.Matsuda, Y.Mizutani, Y.Ohara, and T.Ohga, "Quasi--dc extraction of 70 keV, 5 A ion beam," *Review of Scientific Instruments*, Vol. 51, No. 6, 1980, pp. 728-734.

[7] D.M.Goebel and I.Katz, "*Fundamentals of Electric Propulsion: Ion and Hall Thrusters* ", NASA JPL Space and Technology Series, 2008

[8] P.J.Wilbur, "*Limits on High Specific Impulse Ion Thruster Operation* ", AIAA-2004-4106, 40th AIAA Joint Propulsion Conference, 2009

[9] J.R.Coupland and E.Thompson, "*The Production of High Current, High Quality Beams of Ions and Neutral Particles*", The Review of Scientific Instruments, Vol 42, No 7, 1971

[10] R.Walker et al., " *SAFE/DS4G Thruster Test Report #1* ", ESA ESTEC report ACT-RPT-4100-05-SAFETEST, 2006

[11] R.Walker, C.Bramanti, O.Sutherland, R.Boswell, C.Charles, D.Fearn, J.Gonzalez Del Amo, P.E.Frigot, and M.Orlandi, "*Initial Experiments on a Dual-Stage 4-Grid Ion Thruster for Very High Specific Impulse and Power* ", 42nd AIAA/ASME/SAE/ASEE Joint Propulsion Conference & Exhibit, 2006

[12] M.Coletti, P.Gessini, and S.B.Gabriel, "*A 4-Gridded Ion Engine for High Impulse Mission*", Space Propulsion 2010, San Sebastian, Spain, 2010

[13] J.Kim, J.H.Whealton, and G.Schilling, "*A study of two-stage ion-beam optics*," *Journal of Applied Physics*, Vol. 49, No. 2, 1978, pp. 517-524.

[14] Y.Nakayama and P.J.Wilbur, "*Numerical Simulation of High Specific Impulse Ion Thruster Optics*", 27th International Electric Propulsion Conference, IEPC-01-99, 2001

[15] M.Coletti, P.Gessini, and S.B.Gabriel, "A 4-Gridded Ion Engine for High Impulse Mission", Space Propulsion 2010, San Sebastian, Spain, 2010

[16] C.C.Farnell, J.D.Williams, and P.J.Wilbur, "*Numerical Simulation of Ion Thruster Optics*", 28th International Electric Propulsion Conference, Toulouse, France, 2003

[17] C.C.Farnell, J.D.Williams, and P.J.Wilbur, "*NEXT Ion Optics Simulation via ffx*", NASA/CR-2003-212594, 2003

[18] J.D.Williams, C.C.Farnell, D.A.Laufer, and R.A.Martinez, "HiPEP Ion Optics System Evaluation Using Gridlets", 40th AIAA Joint Propulsion Conference, 2004

[19] M.Coletti and S.B.Gabriel, "*Design of a 4-gridded ion engine for the Hiper project*", 46th AIAA/ASME/SAE/ASEE Joint Propulsion Conference & Exhibit, Nashville, 25-28 July, 2010

[20] M.Coletti and S.B.Gabriel, "*Dual Stage Ion Optics, a Parametric Study*", 42nd AIAA Plasmadynamics and Lasers Conference, Honolulu, USA, 2011

[21] M.Coletti and S.B.Gabriel, "***Dual Stage Ion Optics, a Parametric Study on Performances and Lifetime***", 47th AIAA/ASME/SAE/ASEE Joint Propulsion Conference & Exhibit, San Diego, USA, 31 July - 3 August, 2011

[22] A.J.T.Holmes and E.Thompson, "*Beam steering in tetrode extraction systems*," *Review of Scientific Instruments*, Vol. 52, No. 2, 1981, pp. 172-179.

[23] J.E.Foster, T.Haag, M.Patterson, G.Williams, J.S.Sovey, C.Carpenter, H.Kamhawi, S.Malone, and F.Elliot, "*The High Power Electric Propulsion (HiPEP) Ion Thruster*", NASA/TM-2004-213194, 2004

[24] J.Snyder et al, "*Results of a 2000-Hour Wear Test of the NEXIS Ion Engine*", 29th International Electric Propulsion Conference, Princeton University, 2005

[25] J.Snyder et al, "*Environmental Testing of the NEXT PM1R Ion Engine*", 30th AIAA Fluid Dynamics Conference, Norfolk, VA, June 28-July 1, 2007

[26] S.Kitamura and S.K, "*Overview and Research Status of the JAXA 150-mN Ion Engine*", Acta Astronautica, 61, 2007

[27] http://cs.astrium.eads.net/sp/SpacecraftPropulsion/Rita/RIT-22.html", 2010

[28] H.Leiter et al, "*Extended Performance Evaluation of EADS ST's 200mn Radio Frequency Ion Thruster*", 39th AIAA Joint Propulsion Conference,Huntsville, Alabama, 2003